



# Study of Radiation Levels in the Building Materials of a Historic Monument of Narnaul, Haryana, India

Sanigdha <sup>a\*</sup> and Sunita Dahiya <sup>a</sup>

<sup>a</sup> Department of Physics, Baba Mastnath University, Rohtak, Haryana, 124022, India.

## Authors' contributions

This work was carried out in collaboration between both authors. Both authors read and approved the final manuscript.

## Article Information

DOI: <https://doi.org/10.9734/ijpss/2025/v37i95749>

## Open Peer Review History:

This journal follows the Advanced Open Peer Review policy. Identity of the Reviewers, Editor(s) and additional Reviewers, peer review comments, different versions of the manuscript, comments of the editors, etc are available here: <https://pr.sdiarticle5.com/review-history/144087>

Original Research Article

Received: 28/06/2025  
Published: 20/09/2025

## ABSTRACT

Naturally occurring radioactive materials (NORMs) in building materials can elevate background gamma radiation and pose potential health risks. Establishing baseline radiation levels in historically significant areas is therefore important for both public health and heritage conservation. This study aimed to assess the activity concentration of radionuclides (<sup>226</sup>Ra, <sup>232</sup>Th, and <sup>40</sup>K) and associated radiological hazards in two historical monuments located in Narnaul, Haryana, India—Jal Mahal and Chor Ghumbad and the survey initiated in April 2024. Samples of building materials such as marble, soapstone, brick, and lime were collected from both sites. Each sample was dried, powdered, homogenized, and sealed prior to analysis. Gamma spectrometry using a NaI(Tl) detector was employed to measure activity concentrations, and radiological indices including radium equivalent activity (Raeq), absorbed dose rate (ADR), annual effective dose (AED), excess lifetime cancer risk (ELCR), activity utilization index (AUI), gamma index (I<sub>γ</sub>), and annual gonadal dose equivalent (AGDE) were calculated. The mean activity concentration of NORMs was 518.08 Bq/kg in Jal Mahal and 632.99 Bq/kg in Chor Ghumbad, both

\*Corresponding author: E-mail: [sanigdhayadav18@gmail.com](mailto:sanigdhayadav18@gmail.com);

**Cite as:** Sanigdha, and Sunita Dahiya. 2025. "Study of Radiation Levels in the Building Materials of a Historic Monument of Narnaul, Haryana, India". *International Journal of Plant & Soil Science* 37 (9):731-748. <https://doi.org/10.9734/ijpss/2025/v37i95749>.

higher than the world average of 420 Bq/kg (UNSCEAR). The mean Raeq values were 130.78 Bq/kg and 149.87 Bq/kg for Jal Mahal and Chor Ghumbad, respectively, well below the recommended safety limit of 370 Bq/kg. Similarly, the mean ADR values (60.63 nGy/h and 69.57 nGy/h) were slightly above the global average of 59 nGy/h, while the AED, ELCR, and other indices remained below international safety thresholds.

In conclusion, although both monuments exhibit higher NORM activity concentrations than the global average, for some values the radiological risk indices confirm that the sites are not so hazardous. Continuous monitoring is recommended to ensure long-term safety and preservation of these cultural heritage structures.

*Keywords: Marble; soapstone; radium; gamma radiation; public health.*

## 1. INTRODUCTION

“Natural background radiation is an inseparable component of the Earth’s environment, originating from terrestrial radionuclides, cosmic rays, and atmospheric isotopes. Among these, the terrestrial component—mainly due to the long-lived radionuclides uranium-238 ( $^{238}\text{U}$ ), thorium-232 ( $^{232}\text{Th}$ ), and potassium-40 ( $^{40}\text{K}$ )—is of greatest concern for human exposure” (Kant & Gupta, 2015; Kovler et al., 2017). “These primordial radionuclides and their decay products are distributed unevenly in soils, rocks and building materials, leading to significant variability in radiation levels from region to region” (Abbasi et al., 2020; Malikova et al., 2020). “In areas where geological formations contain higher concentrations of these elements, natural background radiation may exceed international averages, making continuous monitoring essential” (Lolila & Mazunga, 2023; Rene & Akitsu, 2017).

“The presence of gamma-emitting radionuclides in building materials is particularly significant because of prolonged human exposure indoors. Radionuclides from the uranium and thorium series, as well as  $^{40}\text{K}$ , contribute to external gamma radiation, which, in elevated levels, can increase health risks” (Missimer & Teaf, 2019; Patel & Sharma, 2023). “The decay of these isotopes releases alpha, beta, and gamma particles, with gamma rays penetrating deeply and constituting a dominant portion of background dose” (Zanin & Zamirailova, 2016). “In this context, natural radiation studies are important not only for radiation protection but also for environmental management and public health policy” (Shankamma et al., 2022). Numerous investigations have focused on mapping natural radioactivity in soils and construction materials across diverse geographical regions (Del Monte et al., 2024). For instance, Abbasi et al. (2020) reported

elevated activity concentrations in North Cyprus soils, while Malikova et al. (2020) documented uranium and thorium accumulation in Siberian sediments. Similar studies in India have indicated regional variations linked to geology and material use, particularly in Kerala’s high background radiation areas: (Omori et al., 2016). “These findings highlight the necessity of region-specific baseline data to assess health risks and to ensure compliance with international safety guidelines” (UNSCEAR, 2020).

International organizations provide reference values and limits to safeguard populations. The United Nations Scientific Committee on the Effects of Atomic Radiation (UNSCEAR) (2020) reports a global average activity concentration of 420 Bq/kg for  $^{226}\text{Ra}$ ,  $^{232}\text{Th}$ , and  $^{40}\text{K}$  in building materials. The International Commission on Radiological Protection (ICRP, 1993) recommends “an annual effective dose limit of 1 mSv/y for the general public and 20 mSv/y for occupationally exposed workers. Exceeding these limits may contribute to long-term health risks, such as increased lifetime cancer incidence” (Darwish et al., 2015). “To aid comparisons, composite indices like the radium equivalent activity (Raeq) and absorbed dose rate (ADR) are commonly employed, offering standardized measures of radiological hazard” (Delacroix et al., 2002; Martin, 2006; Shapiro, 2002). “Apart from health considerations, natural radioactivity also has implications for industries and construction standards. NORMs occur not only in soils and rocks but also in by-products like fly ash and phosphogypsum, which are widely used in building materials” (Sahoo & Joseph, 2021). “Therefore, understanding the activity levels of radionuclides in construction materials is critical for regulating their safe use, especially in heritage structures where materials are centuries old and may not conform to modern safety standards” (Kovler et al., 2017). The study by Al-Hamarneh and Awadallah (2009) explores

the concentrations of naturally occurring radionuclides- specifically  $^{226}\text{Ra}$ ,  $^{238}\text{U}$ ,  $^{232}\text{Th}$ , and  $^{40}\text{K}$  in the soils of the highlands of northern Jordan, with a focus on evaluating radiation hazards to human health and the environment. Their research provides critical baseline data on soil radioactivity, employing gamma-ray spectrometric analysis to assess both activity concentrations and associated radiation indices, which are essential for understanding background radiation levels and potential risks.

“Studies on environmental radiation emphasize both scientific and societal dimensions. From a public health perspective, quantifying absorbed dose rates and effective doses helps evaluate the risk of genetic damage, reproductive health concerns, and organ-specific exposures” (Rühm et al., 2018). “Excess lifetime cancer risk (ELCR), for example, provides a long-term projection of potential hazards, while indices like the activity utilization index (AUI), gamma index ( $I_\gamma$ ), and annual gonadal dose equivalent (AGDE) are used to estimate risks from building occupancy” (Egidi, 1997; Bossew & Cinelli, 2017). “These indices not only reflect radiation safety but also inform decision-making on resource allocation, zoning, and preservation of historical monuments. Despite global interest, relatively fewer studies address natural radiation in inland historical monuments in India. Most research has been concentrated in regions with mining or coastal exposure” (Al-Khawlany, Khan, & Pathan, 2018; Al-khawlany et al., 2020). “However, inland sites, though less studied, may equally present elevated radiation levels due to local geology and materials. Monuments constructed using locally quarried stone, brick, and lime can contain radionuclides that persist over centuries. As these monuments attract visitors and remain part of community life, assessing their radiological safety is vital” (Musa, 2019; Tye & Milodowski, 2017).

“Narnaul, located in Haryana near the Aravalli mountain range, presents a suitable case study. The region is geologically significant, with diverse lithology including stone and mineral-rich soils. Two monuments in particular—Jal Mahal and Chor Ghumbad—are historically prominent structures dating back to the medieval period. Built from materials such as white marble, soapstone, brick, and lime, they represent both architectural heritage and potential sources of exposure to natural radionuclides. Given the presence of  $^{226}\text{Ra}$ ,  $^{232}\text{Th}$ , and  $^{40}\text{K}$  in such materials, radiation monitoring is necessary for

both public safety and conservation planning. Previous studies emphasize the importance of integrating radiological monitoring with heritage preservation” (Johansson & Steen, 2022; Menon & Kumar, 2019). “Cultural sites are not only tourist attractions but also community spaces, where exposure, though low-level, can be chronic. Hidden health hazards may persist in non-industrial areas, necessitating baseline assessments even where industrial activities are absent” (Khan & Alshukri, 2020; Alwaeli & Mannheim, 2022). “In this study, radiation measurements were performed using a NaI(Tl) gamma-ray spectrometer, a widely applied technique for environmental and building material analysis due to its efficiency and accuracy” (Darwish et al., 2015). “Samples from both Jal Mahal and Chor Ghumbad were collected, processed, and analyzed to determine activity concentrations of  $^{226}\text{Ra}$ ,  $^{232}\text{Th}$ , and  $^{40}\text{K}$ . From these measurements, standard indices such as Raeq, ADR, annual effective dose (AED), ELCR, AUI,  $I_\gamma$ , and AGDE were calculated following internationally recognized methodologies” (UNSCEAR, 2020; ICRP, 1993).

“The results of this investigation provide the first systematic baseline data on soil and building material radioactivity in Narnaul’s monuments. These data are critical not only for assessing immediate health risks but also for informing long-term monitoring strategies. Establishing baseline values allows comparison with future studies and supports risk management policies for heritage sites. Moreover, the findings contribute to broader national and global databases on environmental radiation, strengthening the evidence base for radiation protection frameworks” (Till & Grogan, 2008). Therefore, the objective of this study is to evaluate the activity concentrations of  $^{226}\text{Ra}$ ,  $^{232}\text{Th}$ , and  $^{40}\text{K}$  in the building materials of Jal Mahal and Chor Ghumbad, Narnaul, Haryana, and to assess the associated radiological hazard indices in order to establish reliable baseline data for this historically significant region.

## 2. MATERIALS AND METHOD

Samples of building materials, including white marble, brick, and lime, were collected from two historical monuments—Jal Mahal and Chor Ghumbad in Narnaul, Haryana. To ensure representativeness, samples were manually obtained from different structural portions of the monuments. Each sample was carefully ground, powdered, and homogenized to eliminate

heterogeneity, then oven-dried at 110 °C for two hours to remove residual moisture. The processed materials were subsequently sealed in airtight cylindrical polyethylene containers to prevent radon escape and stored for at least 30 days, allowing secular equilibrium between <sup>226</sup>Ra, <sup>232</sup>Th, and their progeny to be established.

For radiometric analysis, a NaI(Tl) gamma-ray spectrometer with an efficiency of <20% and a resolution of 7% at 661 keV was employed. Each sample was measured for 10,800 seconds to ensure statistical accuracy. Activity concentrations of <sup>226</sup>Ra, <sup>232</sup>Th, and <sup>40</sup>K were determined, and radiological hazard indices were calculated accordingly. The primary aim of this study was to determine indoor and outdoor background radiation dose rates and to estimate the Radium Equivalent Activity (Raeq), Absorbed Dose Rate (ADR), Annual Effective Dose (AED), Activity Utilization Index (AUI), Gamma Index, Excess Cancer Risk, Effective Dose Rate (ELCR) to whole body organ, Annual gonadal dose equivalent to the residents of their nearby area in Narnaul. The <sup>222</sup>Rn mass exhalation rate (Jm) from building materials was calculated using the growth data fitted into the following equation

$$C(t) = C(t) = J_m M / \Lambda V (1 - e^{-\Lambda t}) + C_R e^{-\Lambda t} \quad (\text{Sahoo et al., 2007})$$

where C(t) is the radon concentration (Bq m<sup>-3</sup>) inside the chamber at time t, C<sub>R</sub> is the background radon concentration (Bq m<sup>-3</sup>), J<sub>m</sub> is the radon mass exhalation rate (Bq kg<sup>-1</sup> h<sup>-1</sup>), M is the total mass of the building material sample (kg), V is the volume of the chamber (m<sup>3</sup>),  $\Lambda$  is

the decay constant of <sup>222</sup>Rn, and t is the accumulation time. The <sup>220</sup>Rn (thoron) surface exhalation rate (J<sub>s</sub>) for building materials was calculated as

$$J_S = C_T V_T \Lambda / A \quad (\text{Sahoo et al., 2014; Kanse et al., 2013})$$

where C<sub>T</sub> is the average thoron concentration inside the chamber (Bq m<sup>-3</sup>), V is the residual air volume of the chamber (m<sup>3</sup>),  $\Lambda$  is the decay constant of <sup>220</sup>Rn, and A is the exposed surface area of the building material sample (m<sup>2</sup>).

## 2.1 Study Area

Haryana located in north-western region of India (27°39'–30°35'N latitude and 74°28'–77°28' longitude), served as the study site. Two ancient monuments, Jal Mahal and Chor Ghumbad both selected from Narnaul (28.1920 °N, 76.6191°E). Narnaul is historically significant town, established during the 12<sup>th</sup> century, situated near the Aravalli mountain range. The region is characterized by a hot, dry climate and sandy plains with numerous dunes. Local construction materials traditionally include stone, bricks, lime.

## 2.2 Measurement Technique

For radiation measurement, samples from ancient buildings were analyzed using a NaI (sodium iodide) gamma-ray spectrometer. The detector was specifically chosen to assess the health impacts of ancient building material decay radiation.

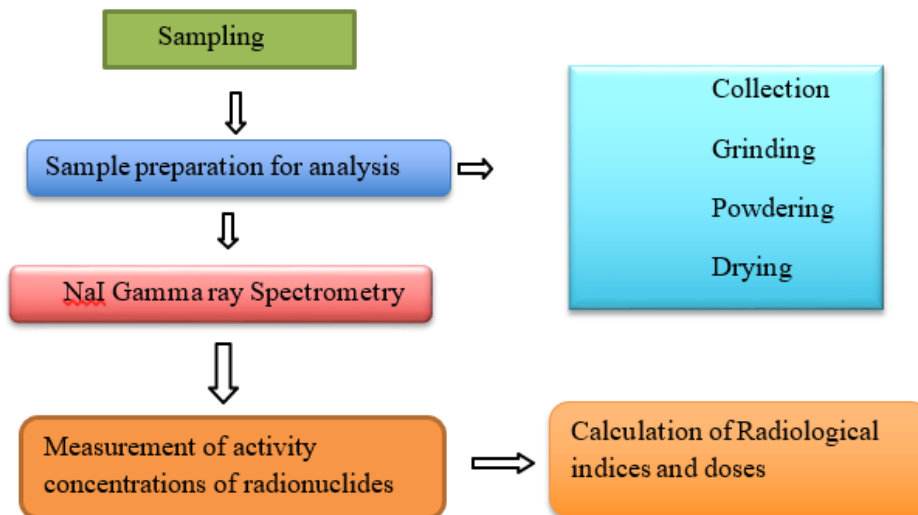


Chart 1. Sampling method



**Fig. 1. Representing the NaI gamma ray spectrometer**

Specifications of the NaI (TI) Detector are-

**Type:** Sodium iodide (NaI(Tl)) scintillation detector (Darwish et al., 2015).

**Crystal size:** 63 mm x 63 mm (Delacroix et al., 2002).

**Energy resolution:** ~7% at 661 keV for  $^{137}\text{Cs}$  with ~9 kBq activity (Darwish et al., 2015).

**Energy detection range:** 50 keV – 3 MeV (Delacroix et al., 2002).

**Relative efficiency:** <20% (Darwish et al., 2015).

**Minimum detectable activity (MDA):**

$^{226}\text{Ra}$ : ~3 Bq/kg

$^{232}\text{Th}$ : ~3 Bq/kg

$^{40}\text{K}$ : ~30 Bq/kg (Delacroix et al., 2002). Counting time per sample: 10,800 seconds (~3 hours) (Darwish et al., 2015). Spectrum analysis software: SPTR-ATC (AT-1315), using multichannel analyzer (MCA) output for peak identification (Delacroix et al., 2002).

Research potential of NaI Detector are as follows-

1. Regulatory Bodies – Evaluation of radionuclide concentrations ( $^{226}\text{Ra}$ ,  $^{232}\text{Th}$ ,  $^{40}\text{K}$ ) in soils and corresponding construction material.
2. Cement Industry – Assessment of fly ash addition in cement.
3. Food Industry – Measurement of natural radionuclides in dry, powdered food products.

All dose rates were recorded from detector display and used to calculate activity concentration.

The Radium Equivalent Dose ( $R_{\text{aeq}}$ ) of background radiation was estimated as

$$R_{\text{aeq}} = 0.077A_{\text{K}} + A_{\text{Ra}} + 1.43A_{\text{Th}} \quad (\text{Bq/kg}) \quad - \text{Beretka \& Mathew (1985)}$$

The total Absorbed Dose Rate (ADR) was estimated as

$$\text{ADR} = 0.0417 A_{\text{K}} + 0.462 A_{\text{Ra}} + 0.604 A_{\text{Th}} \quad (\text{nGy/h}) \quad - \text{UNSCEAR. (2000)}$$

Here,  $R_{\text{aeq}}$  (Bq/kg) is expression of the specific activities of  $^{226}\text{Ra}$ ,  $^{232}\text{Th}$ , and  $^{40}\text{K}$  by a single quantity, which takes into account the radiation hazards associated with radon and its progeny. The ADR is total Absorbed Dose Rate calculations are expressed in nGy/h per 1 Bq/kg,  $A_{\text{K}}$  is the activity of  $^{40}\text{K}$  of the analyzed material, measured as the number of spontaneous nuclear transformations of the  $^{40}\text{K}$  radionuclide per sec. The  $A_{\text{Ra}}$  is the activity of  $^{226}\text{Ra}$  of the analyzed material, measured as the number of spontaneous nuclear transformations of the  $^{226}\text{Ra}$  radionuclide per sec. The  $A_{\text{Th}}$  is the activity of  $^{232}\text{Th}$  of the analyzed material, measured as the number of spontaneous nuclear transformations of the  $^{232}\text{Th}$  radionuclide per sec.

The Annual Effective dose (AED) was estimated by using the formula

$$\text{AED} (\text{mSv/y}) = \text{ADR} \times 8760 \times 10^{-6} \times 0.2 \times 0.7 \quad (\text{svGy}^{-1}) \quad - \text{UNSCEAR. (2000)}$$

The annual effective dose equivalent is used to estimate the health risk associated with exposure of an individual. To calculate the AED the conversion factor (0.7) and occupancy factor has been used to convert absorbed dose rate to human effective dose equivalent with an occupancy of 20%. The calculated Radium Equivalent Dose ( $R_{\text{aeq}}$ ), total Absorbed Dose Rate (ADR), and annual effective dose rate for all the samples (both historic places) are given in Tables 2, 3 with their mean values. The world average value of ADR is 84 nGy/h and the world average value of AED is 0.52 mSv/y. The

International Commission on Radiological Protection (ICRP) has recommended the annual effective dose equivalent limit of 1 mSv/yr for the individual members of the public and 20 mSv/yr for radiation workers [International Commission on Radiological Protection (ICRP) , 1993].

**Table 1. Introduction of types of samples**

Sr.no	Name of sample	Types of sample	Initialization of samples
1	Jal Mahal -1	White Marble	JMN-1
2	Jal Mahal -2	Soap Stone	JMN-2
3	Jal Mahal -3	Brick	JMN-3
4	Jal Mahal -4	Lime	JMN-4
5	Chor Ghumbad-5	Lime	CGN-5
6	Chor Ghumbad-6	White stone	CGN-6
7	Chor Ghumbad-7	Brick	CGN-7

**Table 2. Sample calculation of jal mahal building material Req, ADR, AED By using activity concentrations**

Sample	Activity Concentration			Radium equivalent activity (Raeq) (Bq/Kg)	Absorbed Dose Rate (ADR) nGy/h	Annual Effective Dose (AED)*10 <sup>-6</sup> (mSv/y)
	<sup>226</sup> Ra(Bq/Kg)	<sup>232</sup> Th(Bq/Kg)	<sup>40</sup> K(Bq/Kg)			
JMN-1	25	21	325	80.05	37.786	46341.36
	28	24	329	87.65	41.151	50467.954
	32	27	332	96.17	44.936	55110.00
JMN-2	30	58	798	174.38	82.168	100771.57
	33	61	801	181.90	85.491	104847.02
	36	64	805	189.50	88.856	108973.61
JMN-3	28	35	268	98.68	45.251	55496.562
	30	39	270	106.5	48.67	59695.020
	33	42	273	114.08	51.998	63770.469
JMN-4	43	48	357	139.12	63.744	78176.745
	45	51	359	145.57	66.564	81634.457
	49	55	363	155.60	70.995	87068.390
MEAN	34.33	43.75	440	130.775	60.63	74362.764

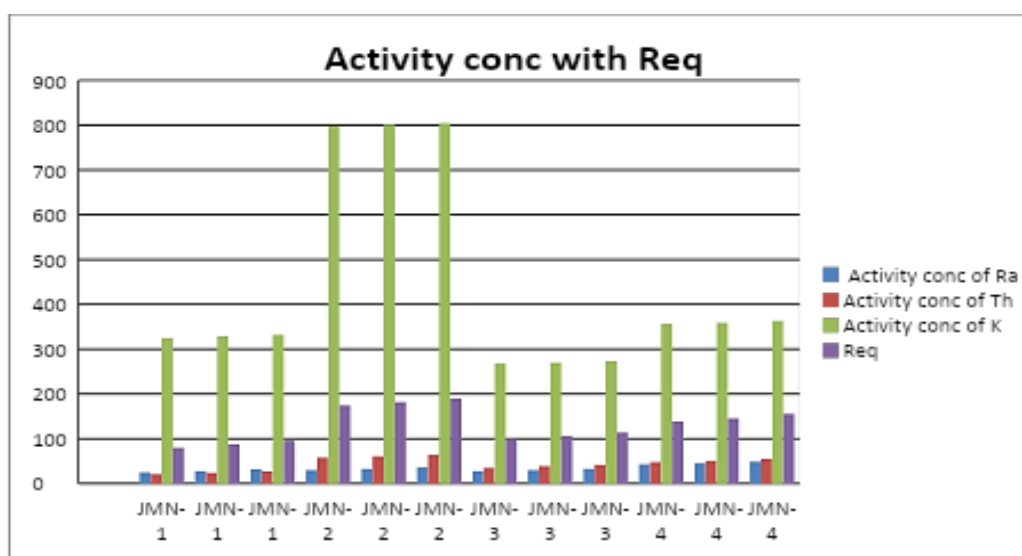


**Fig. 2. Graphical representation of jal mahal activity concentrations with radium equivalent activity (Raeq)**

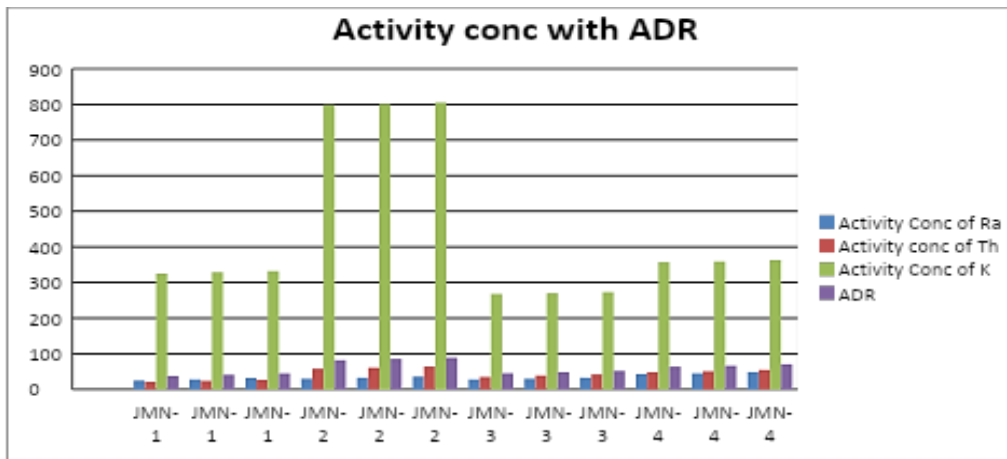


Fig. 3. Graphical representation of jal mahal activity concentrations with absorbed dose rate (ADR)

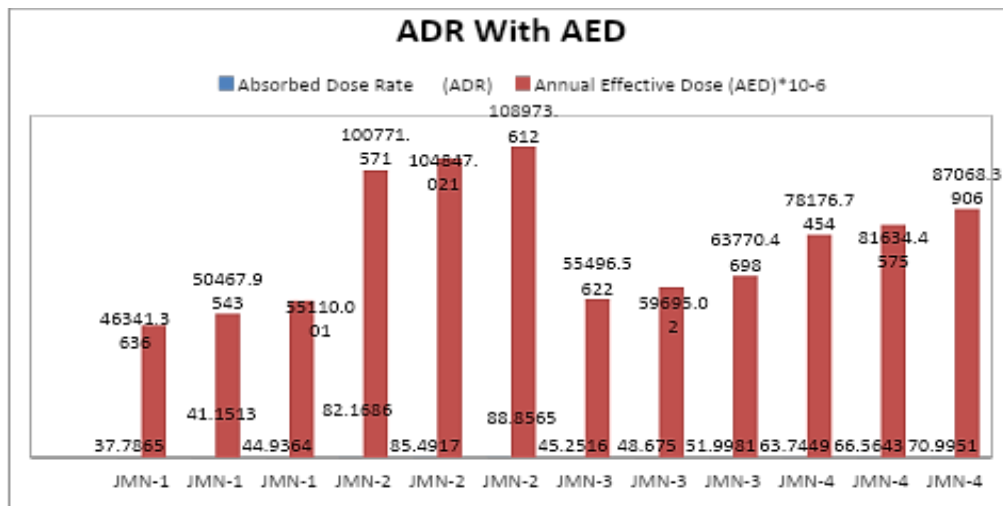


Fig. 4. Graphical representation of jal mahal absorbed dose rate (ADR) with annual effective dose (AED)

Table 3. Sample calculation of chor ghumbad building material R<sub>aeq</sub>, ADR, AED by using activity concentrations

Sample	Activity Concentration	Radium equivalent activity (R <sub>aeq</sub> ) (Bq/Kg)	Absorbed Dose Rate (ADR) (nGy/h)	Annual Effective Dose (AED) × 10 <sup>-6</sup> (mSv/y)
	<sup>226</sup> Ra(Bq/Kg) <sup>232</sup> Th(Bq/Kg) <sup>40</sup> K(Bq/Kg)			
	34                      39                      348	116.56	53.775	65950.39
CGN-5	37                      41                      351	122.65	56.494	69285.10
	40                      44                      355	130.25	59.859	73411.69
	31                      59                      801	177.04	83.359	102232.33
CGN-6	35                      62                      803	185.49	87.103	106823.24
	38                      65                      806	193.01	90.426	110898.69
	19                      54                      488	133.79	61.743	75722.35
CGN-7	22                      57                      490	141.24	65.02	79746.6
	25                      60                      493	148.76	68.348	83822.10
MEAN	31.22222              53.444                      548.333	149.86	69.570	85321.39

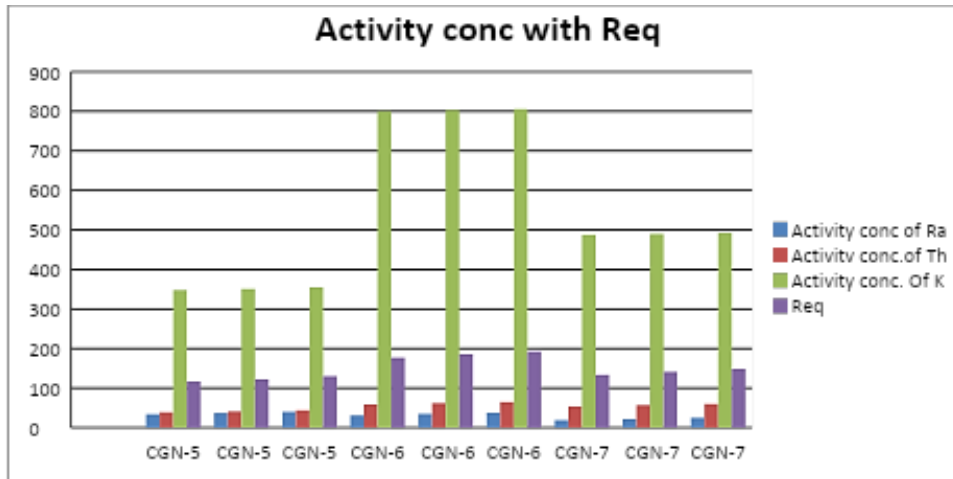


Fig. 5. Graphical representation of chor ghumbad activity concentrations with radium equivalent activity (Req)

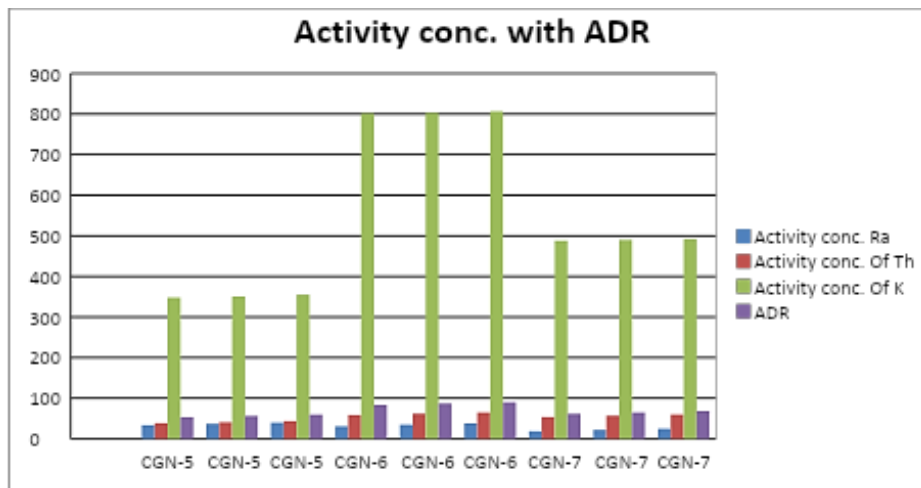


Fig. 6. Graphical representation of chor ghumbad activity concentrations with absorbed dose rate (ADR)

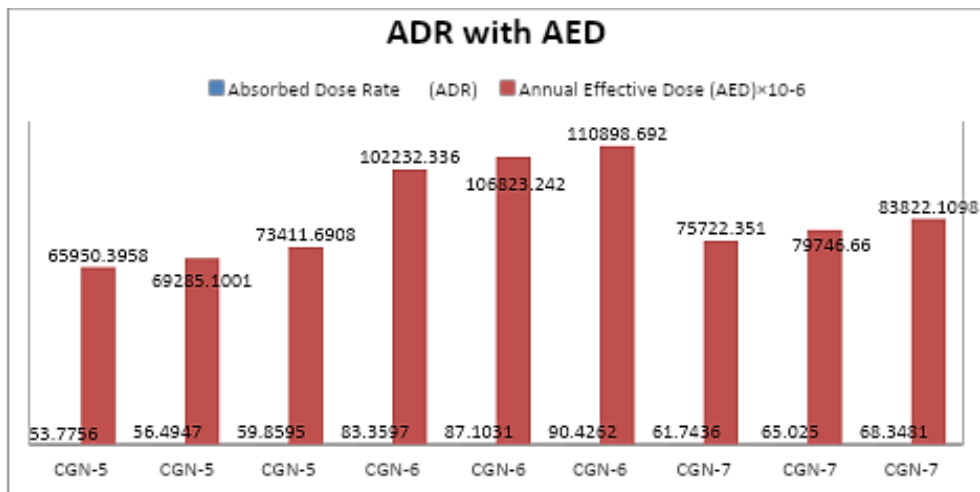


Fig. 7. Graphical representation of chor ghumbad activity concentrations with annual effective dose (AED)

The Excess Life Time cancer Risk (ELCR) was estimated by using the formula

$$ELCR = AED \times LE \times RE \text{ - ICRP. (1991).}$$

$$ELCR = AED \times 70 \times 0.05$$

The Effective dose rate Dorgans (Dorg) was derived by equation

$$Dorgans = AED \times f$$

$$Dorgans \text{ (whole body)} = AED \times 0.68$$

The excess life time cancer risk is estimation of the potential of cancer development over a lifetime, caused by irradiation from historic building materials. ELCR was calculated based upon values of AED, LE and RE; where LE is life

expectancy (70) years and RF is fatal risk factor per Sievert, that is 0.05. The annual effective dose equivalent represents the degree of genetic significance of the annual dose that the reproductive organs of a population receive.

Organs with rapidly dividing cells, such as gonads, active bone marrow cells, lungs, testes, ovaries and bone surface cells, are considered interesting by the UN Scientific Committee on the Effects of Atomic Radiation. The effective dose rate Dorgans is delivered to a particular organ the mean energy absorbed per unit mass averaged over the entire tissue or organ can be calculated using the formula. Where f is the conversion factor of organ dose from air dose. The conversion factor for lungs, ovaries, bone marrow, testes and the whole body are 0.64, 0.58, 0.69, 0.82, 0.68, respectively.

**Table 4. AED, ELCR, D<sub>organ</sub> calculated values of Jal Mahal**

Sample	Annual Effective Dose (AED) × 10 <sup>-6</sup> (mSv/y)	Excess Lifetime Cancer Risk (ELCR) × 10 <sup>-6</sup>	Dose Rate of Body Organs (D <sub>organ</sub> ) × 10 <sup>-6</sup> (mSv/y)
JMN-1	46341.36	162194.77	31512.12
	50467.954	176637.84	34318.20
	55110.00	192885.00	37474.80
	100771.57	352700.49	68524.66
JMN-2	104847.02	366964.57	71295.97
	108973.61	381407.64	74102.05
	55496.562	194237.96	37737.66
JMN-3	59695.02	208932.57	40592.61
	63770.46	223196.64	43363.91
	78176.74	273618.60	53160.18
JMN-4	81634.45	285720.60	55511.43
	87068.39	304739.36	59206.50
Mean	74362.76	260269.67	50566.679

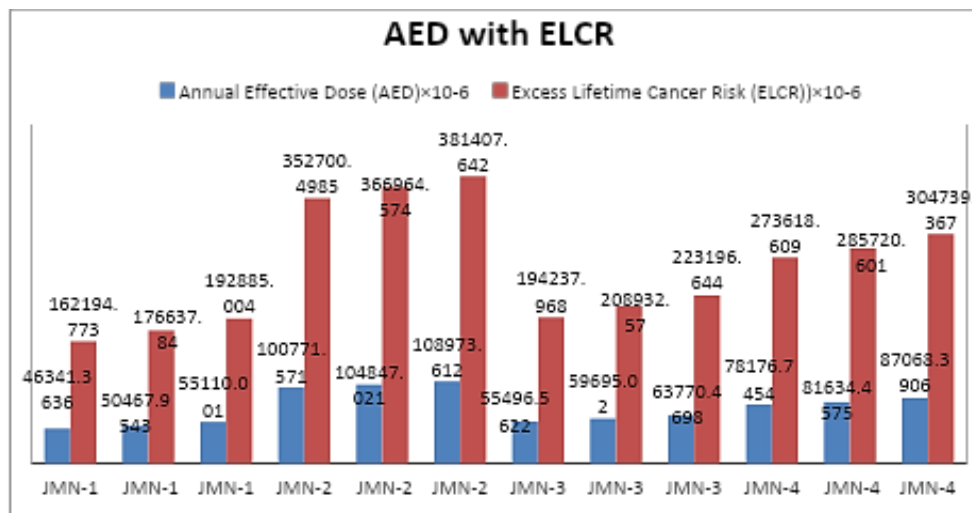


**Fig. 8. Graphical representation of Jal Mahal annual effective dose (AED) with excess life time cancer risk (ELCR)**

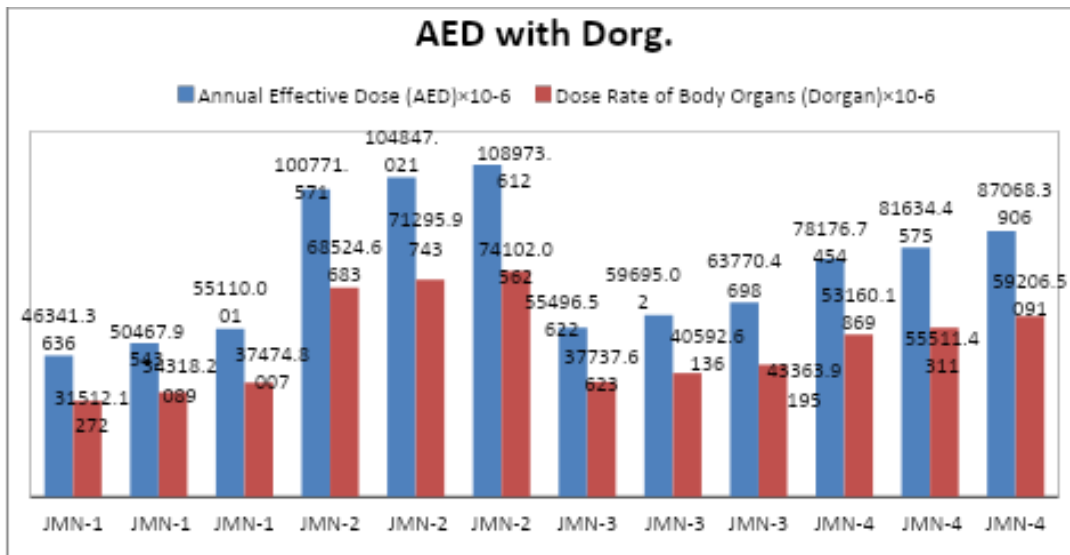


Fig. 9. Graphical representation of Jal Mahal annual effective dose (AED) with dose rate of body organ (Dorg)

Table 5. AED, ELCR,  $D_{organ}$  calculated values of chor ghumbad

Sample	Annual Effective Dose (AED) × 10 <sup>-6</sup> (mSv/y)	Excess Lifetime Cancer Risk (ELCR) × 10 <sup>-6</sup>	Dose Rate of Body Organs ( $D_{organ}$ ) × 10 <sup>-6</sup> (mSv/y)
CGN-5	65950.39	230826.38	44846.26
	69285.10	242497.85	47113.86
	73411.69	256940.91	49919.94
	102232.33	357813.17	69517.98
CGN-6	106823.24	373881.34	72639.80
	110898.69	388145.42	75411.11
	75722.35	265028.22	51491.19
CGN-7	79746.66	279113.31	54227.72
	83822.10	293377.38	56999.03
Mean	85321.39	298624.89	58018.55

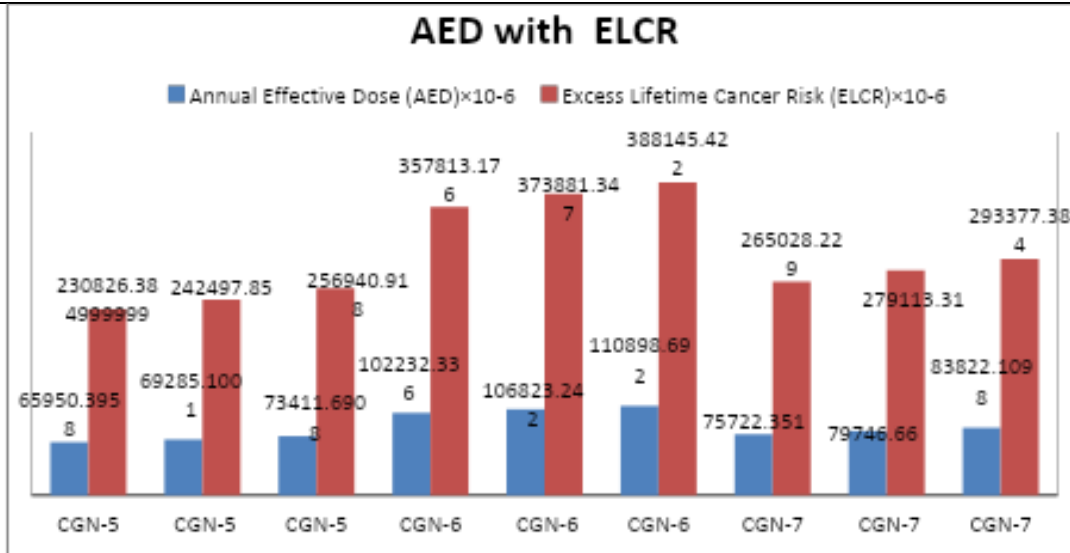


Fig. 10. Graphical representation of Chor Ghumbad annual effective dose (AED) with excess life time cancer risk (ELCR)

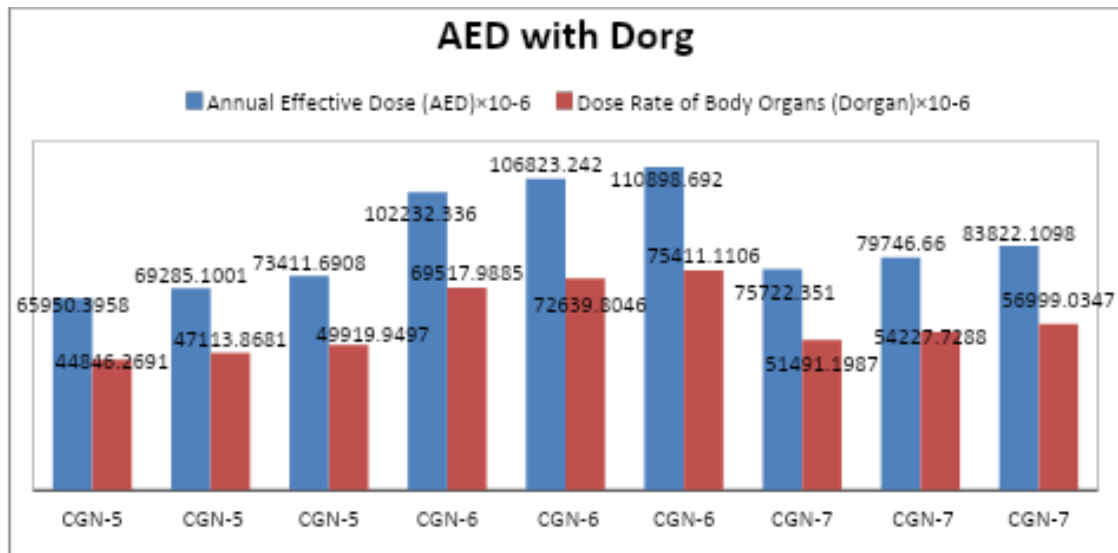


Fig. 11. Graphical representation of Chor Ghumbad annual effective dose (AED) with dose rate of body organ (Dorg.)

Table 6. AUI ,I<sub>γ</sub>, AGDE calculated data of Jal Mahal

Sample	Activity concentration (Bq/Kg)			Activity Utilization Index (AUI)	Gamma Index Factor (I <sub>γ</sub> )	Annual Gonadal Dose Equivalent (AGDE) μSv/y
	<sup>226</sup> Ra	<sup>232</sup> Th	<sup>40</sup> K			
JMN-1	25	21	325	0.5274	0.29666	267.08
	28	24	329	0.5646	0.323	290.14
	32	27	332	0.6024	0.3523	315.98
	30	58	798	1.3060	0.656	585.71
JMN-2	33	61	801	1.3423	0.682	608.46
	36	64	805	1.3795	0.7083	631.53
	28	35	268	0.6165	0.35766	316.97
JMN-3	30	39	270	0.6599	0.385	340.5
	33	42	273	0.6962	0.411	363.252
	43	48	357	0.8437	0.50233	445.60
JMN-4	45	51	359	0.8775	0.52466	464.95
	49	55	363	0.9259	0.5593	495.29
Mean	34.3333	43.7500	440.000	0.86187	0.47986	427.124

The Activity Utilization index (AUI) estimation of total dose rates in air from naturally occurring radionuclides in building materials, calculated from activity concentration measurements of the material Activity Utilization index (AUI) was estimated by using the formula

$$AUI = \frac{ARa}{50 \text{ Bq/kg}} \times 0.0809 + \frac{Ath}{50 \text{ Bq/kg}} \times 0.4798 + \frac{AK}{500 \text{ Bq/kg}} \times 0.4392$$

where the values 0.0809, 0.4798, and 0.4392 represent fractional percentages of the total dose from <sup>226</sup>Ra, <sup>232</sup>Th, and <sup>40</sup>K ( $f_{Ra} = 8.09\%$ ,  $f_{Th} =$

$47.98\%$ , and  $f_K = 43.92\%$ )- European Commission. (1999)

The gamma activity concentration I<sub>γ</sub> estimation of the gamma radiation hazard associated with the radionuclides inside of the building materials, calculated from activity concentration measurements of the material has been defined by the European Commission according to Formula

$$I_{\gamma} = \frac{AK}{3000 \text{ Bq/kg}} + \frac{ARa}{300 \text{ Bq/kg}} + \frac{Ath}{200 \text{ Bq/kg}} - \text{European Commission. (1999).}$$

The Annual Gonadal dose equivalent (AGDE) in  $\mu\text{Sv/y}$  is evaluation for the potential effects of the specific activities of  $^{226}\text{Ra}$ ,  $^{232}\text{Th}$ , and  $^{40}\text{K}$  on certain important organs, such as reproductive organs (gonads), bone marrow, and bone cells.  $A_K$  is the activity of  $^{40}\text{K}$  of the analysed material, measured as the number of spontaneous nuclear transformations of the  $^{40}\text{K}$  radionuclide per sec. The  $A_{\text{Ra}}$  is the activity of  $^{226}\text{Ra}$  of the analyzed

material, measured as the number of spontaneous nuclear transformations of the  $^{226}\text{Ra}$  radionuclide per sec. The  $A_{\text{Th}}$  is the activity of  $^{232}\text{Th}$  of the analyzed material, measured as the number of spontaneous nuclear transformations of the  $^{232}\text{Th}$  radionuclide per sec.

$$\text{AGDE} = 3.09 A_{\text{Ra}} + 4.18 A_{\text{Th}} + 0.314 A_K \text{ (}\mu\text{Sv/y)}$$

Mamont-Ciesla et al., (1982)

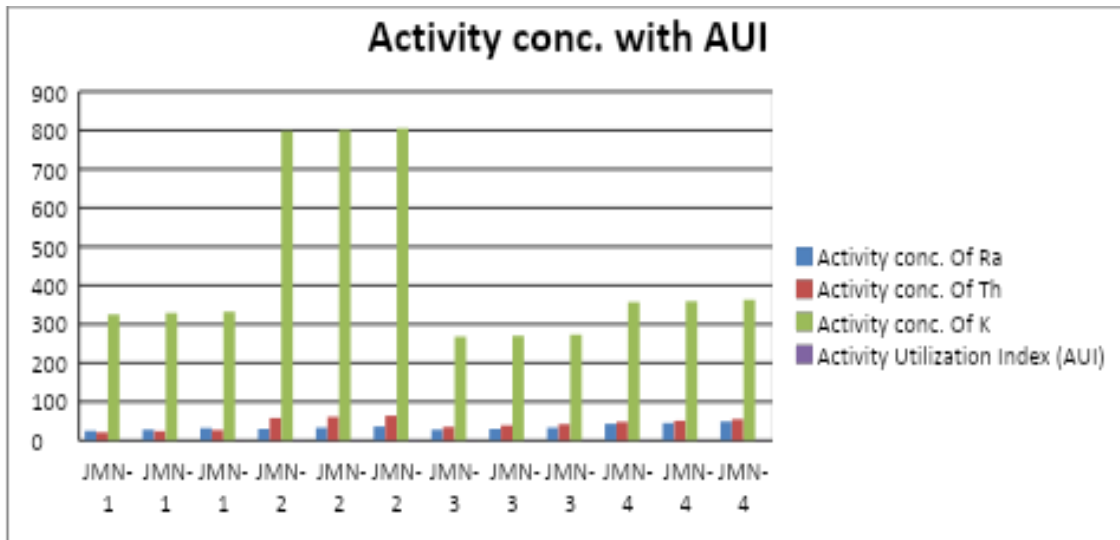


Fig. 12. Graphical representation of Jal mahal activity concentrations with activity utilization index (AUI)

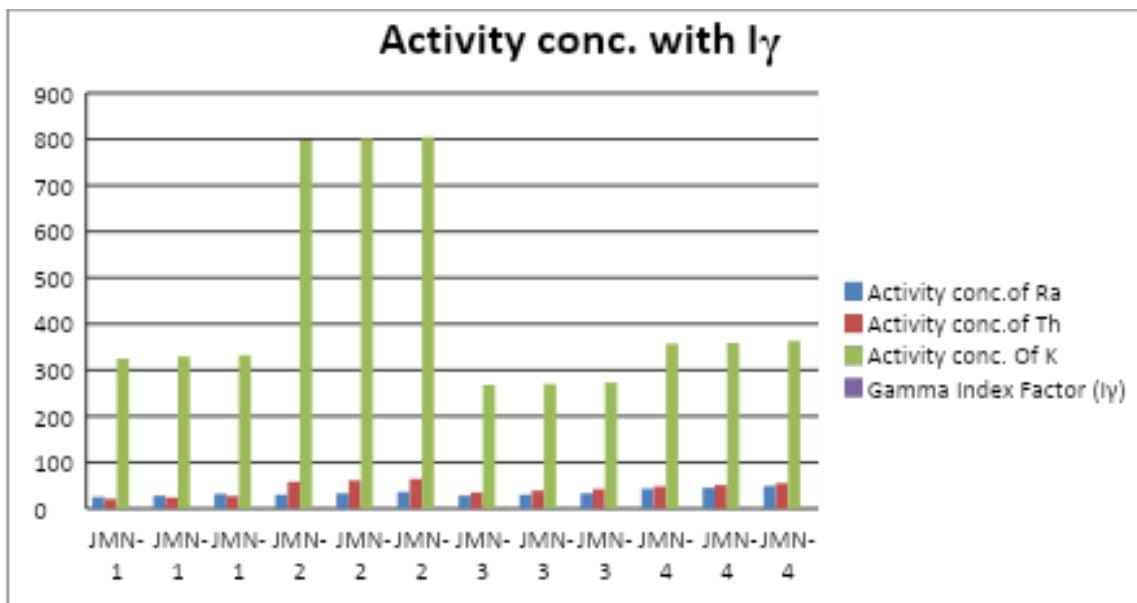


Fig. 13. Graphical representation of Jal Mahal activity concentrations with gamma index factor ( $I_\gamma$ )

Table 7. AUI , I<sub>γ</sub>,AGDE calculated data Chor Ghumbad

Sample	Activity Concentration (Bq/Kg)			Activity Utilization Index (AUI)	Gamma Index Factor (I <sub>γ</sub> )	Annual Gonadal Dose Equivalent (AGDE) μSv/y
	<sup>226</sup> Ra(Bq/Kg)	<sup>232</sup> Th(Bq/Kg)	<sup>40</sup> K(Bq/Kg)			
CGN-5	34	39	348	0.734	0.424	377.35
	37	41	351	0.761	0.445	395.92
	40	44	355	0.798	0.471	418.99
CGN-6	31	59	801	1.3199	0.665	593.92
	35	62	803	1.356	0.694	619.45
	38	65	806	1.39	0.720	642.20
CGN-7	19	54	488	0.97	0.496	437.66
	22	57	490	1.012	0.521	460.1
	25	60	493	1.049	0.547	473.582
mean	31.2222	53.4444	548.333	1.0450	0.554	491.021

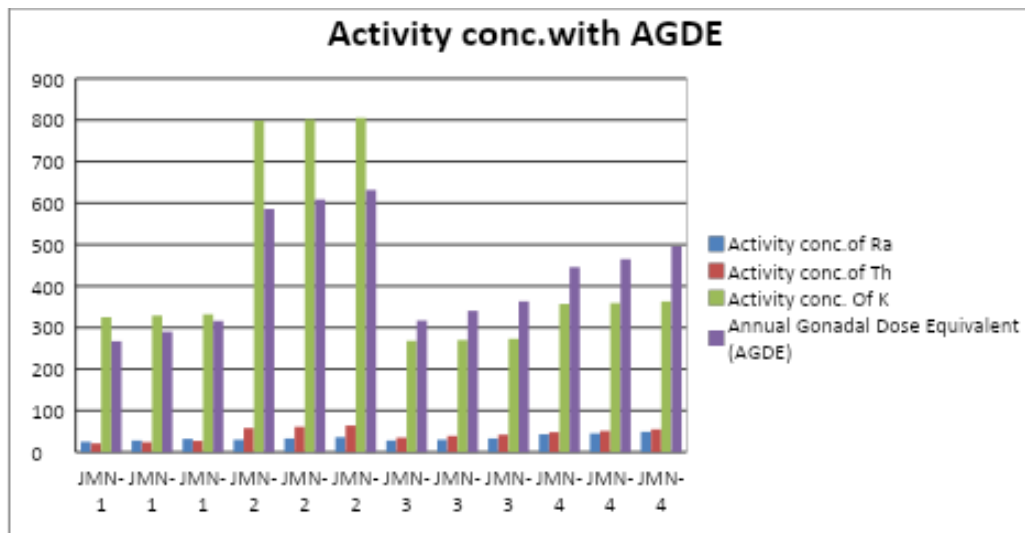


Fig. 14. Graphical representation of Jal Mahal activity concentrations with annual gonadal dose equivalent (AGDE)

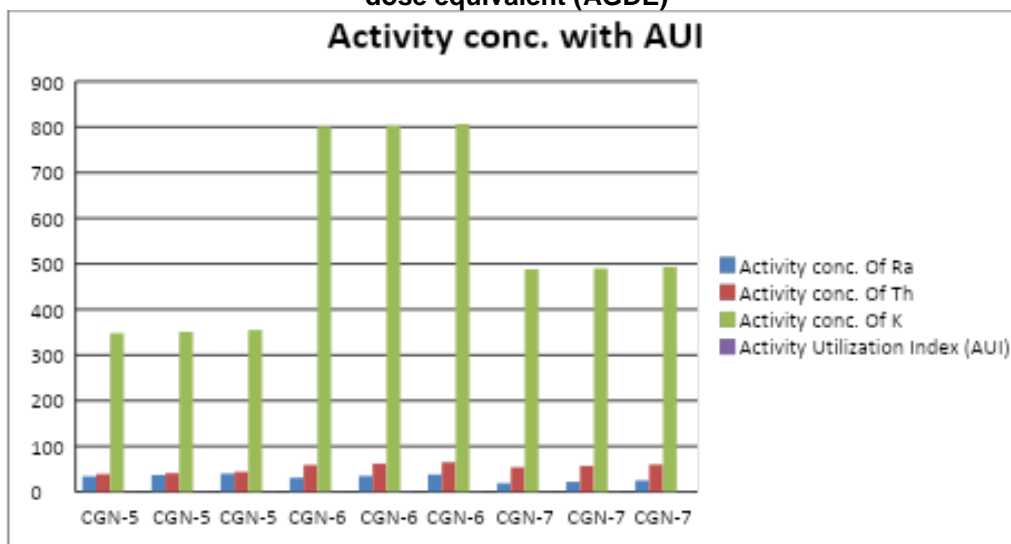


Fig. 15. Graphical representation of Chor Ghumbad activity concentrations with activity utilization index (AUI)

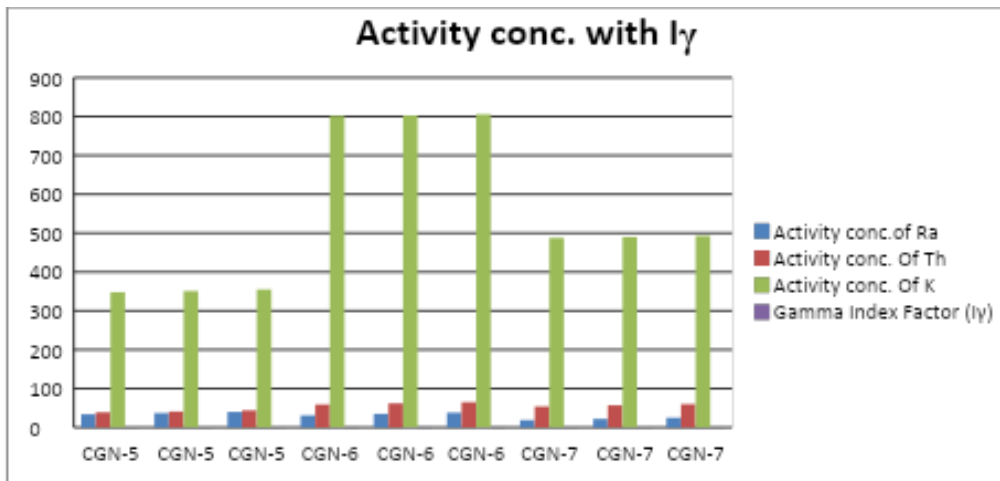


Fig. 16. Graphical representation of Chor Ghumbad activity concentrations with gamma index factor ( $I_\gamma$ )

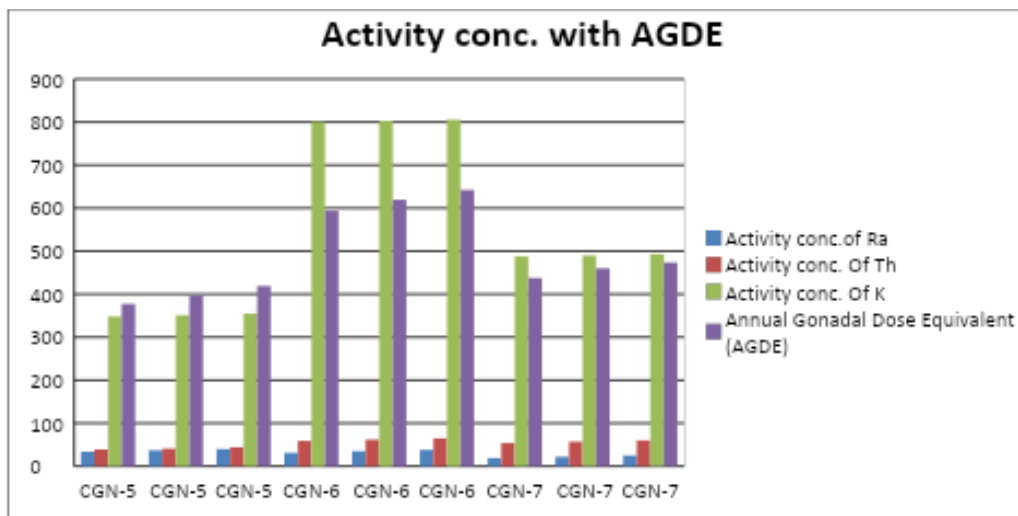


Fig. 17. Graphical Representation of Chor Ghumbad activity concentrations with annual gonadal dose equivalent (AGDE)

### 3. RESULTS

For Jal Mahal, activity concentration of radionuclides ranged between 25-49 Bq/kg for  $^{226}\text{Ra}$ , 21-64 Bq/kg for  $^{232}\text{Th}$  and 268-805 Bq/kg for  $^{40}\text{K}$ , with mean values of 34.33, 43.75 and 440 Bq/kg, respectively. The mean radium equivalent activity ( $R_{\text{eq}}$ ) was 130.78 Bq/kg, the absorbed dose rate (ADR) was 60.63 nGy/h, and the annual effective dose (AED) was 0.074 mSv/y. For Chor Ghumbad, radionuclide activity ranged from 19–40 Bq/kg for  $^{226}\text{Ra}$ , 39–65 Bq/kg for  $^{232}\text{Th}$ , and 348–806 Bq/kg for  $^{40}\text{K}$ , with mean values of 31.22, 53.44, and 548.33 Bq/kg, respectively. The mean  $R_{\text{eq}}$  was 149.87 Bq/kg, ADR 69.57 nGy/h, and AED 0.085 mSv/y. The Excess Lifetime Cancer Risk (ELCR) ranged

from  $1.62 \times 10^{-4}$  to  $3.81 \times 10^{-4}$ , with a mean of  $2.60 \times 10^{-4}$  for Jal Mahal. For Chor Ghumbad, the ELCR ranged from  $2.30 \times 10^{-4}$  to  $3.88 \times 10^{-4}$ , with a mean of  $2.99 \times 10^{-4}$ . Both averages are lower than the global mean value of  $1.45 \times 10^{-3}$  reported by UNSCEAR.

The effective organ dose ( $D_{\text{organ}}$ ) for Jal Mahal samples ranged between  $3.15 \times 10^{-2}$  mSv/y and  $7.41 \times 10^{-2}$  mSv/y, with a mean of  $5.06 \times 10^{-2}$  mSv/y. For Chor Ghumbad, the values ranged from  $4.48 \times 10^{-2}$  mSv/y to  $7.54 \times 10^{-2}$  mSv/y, with a mean of  $5.80 \times 10^{-2}$  mSv/y. These are considerably below the ICRP recommended annual limit of 1 mSv/y for the general public. The Activity Utilization Index (AUI) for Jal Mahal ranged between 0.52–1.38 (mean: 0.86), while

for Chor Ghumbad it ranged from 0.73–1.39 (mean: 1.05), both values being below the recommended safe limit of 2. Similarly, the Gamma Index ( $I_\gamma$ ) values for Jal Mahal (0.30–0.71, mean: 0.48) and Chor Ghumbad (0.42–0.72, mean: 0.55) did not exceed the restricted limit of 1.

The Annual Gonadal Dose Equivalent (AGDE) ranged from 267.08–631.53  $\mu\text{Sv/y}$  (mean: 427.12  $\mu\text{Sv/y}$ ) for Jal Mahal, and 377.35–642.20  $\mu\text{Sv/y}$  (mean: 491.02  $\mu\text{Sv/y}$ ) for Chor Ghumbad. These values fall within the reported global range of 300–520  $\mu\text{Sv/y}$  for building materials. In summary, while the total activity concentrations in Jal Mahal (518.08 Bq/kg) and Chor Ghumbad (632.99 Bq/kg) exceed the world average of 420 Bq/kg, all calculated radiological indices—including Raeq, ADR, AED, ELCR, AUI,  $I_\gamma$ , and AGDE—remain within internationally accepted safety limits.

## 4. DISCUSSION

The radiological assessment of Jal Mahal and Chor Ghumbad reveals that the average Annual Effective Dose (AED) values, 0.074 mSv/y and 0.085 mSv/y respectively, are substantially lower than the global average of 0.52 mSv/y and remain well within the ICRP-60 recommended threshold. Correspondingly, the Excess Lifetime Cancer Risk (ELCR) and Dorgan indices also fall below worldwide reference levels, affirming negligible radiological health hazards. The mean Activity Utilization Index (AUI) values, 0.862 for Jal Mahal and 1.045 for Chor Ghumbad, remain below the prescribed safety limit, although select samples (JMN-2 and CGN-6) approach the permissible boundary. Similarly, the mean gamma index ( $I_\gamma$ ) values, 0.480 and 0.554, are within the acceptable restriction of  $I_\gamma = 1$ , with isolated readings nearing the critical threshold. Furthermore, the mean Annual Gonadal Dose Equivalent (AGDE) values of 427.12  $\mu\text{Sv/y}$  (Jal Mahal) and 491.02  $\mu\text{Sv/y}$  (Chor Ghumbad) reinforce the overall compliance with international radiological safety standards.

### 4.1 Comparison with World Averages

The results reveal that radionuclide activity concentrations in both Jal Mahal and Chor Ghumbad exceed the global average value of 420 Bq/kg for building materials. However, the calculated radiological indices remain within internationally accepted safety limits. The mean Raeq values of 130.78 Bq/kg (Jal Mahal) and 149.87 Bq/kg (Chor Ghumbad) are well below

the UNSCEAR threshold of 370 Bq/kg. Similarly, the mean AED values of 0.074 mSv/y and 0.085 mSv/y are significantly lower than the ICRP recommended annual exposure limit of 1 mSv/y for the public. These findings confirm that both sites are radiologically safe despite elevated activity concentrations.

### 4.2 Health Implications

The slightly higher absorbed dose rates compared to the world average of 59 nGy/h (60.63 nGy/h for Jal Mahal and 69.57 nGy/h for Chor Ghumbad) suggest the need for continued monitoring. Nevertheless, the estimated Excess Lifetime Cancer Risk (ELCR) values are substantially below the global average of  $1.45 \times 10^{-3}$ , indicating minimal long-term health risks. The effective organ dose values also remain far below the safety criterion, reinforcing the conclusion that exposure to radiation from these monuments does not pose significant hazards to visitors or residents in the surrounding areas.

### 4.3 Significance for Heritage Sites

The assessment of radiological indices, including AUI,  $I_\gamma$ , and AGDE, further demonstrates that the building materials of these historic monuments pose no notable radiological hazard. This outcome is vital for both public health and cultural preservation. Since Narnaul's monuments are of historical and cultural importance, establishing baseline radiation levels contributes to their safe usage, sustainable conservation, and enhanced public awareness of environmental radiation. Regular monitoring of such sites is recommended to safeguard community health, ensure responsible use of natural resources, and protect heritage structures for future generations.

## 5. CONCLUSION

This study establishes important baseline data on natural radioactivity levels in the historic monuments of Narnaul, Haryana. Although the activity concentrations of radionuclides in Jal Mahal and Chor Ghumbad were found to be higher than the global average, the calculated radiological indices—including Raeq, ADR, AED, ELCR, AUI,  $I_\gamma$ , and AGDE—remained within internationally permissible limits. These results indicate that the monuments do not pose any immediate health risks to visitors or residents in the surrounding areas.

The significance of this work lies not only in its scientific contribution but also in its practical importance for society. Radiation is an invisible environmental factor that can affect human health, and therefore continuous monitoring of such sites is essential. By linking public safety with cultural preservation, this study underscores the value of responsible environmental management. Ultimately, the findings provide guidance for ensuring safe living conditions while safeguarding historical monuments for future generations.

#### DISCLAIMER (ARTIFICIAL INTELLIGENCE)

Authors hereby declare that NO generative AI technologies such as Large Language Models (ChatGPT, COPILOT, etc) and text-to-image generators have been used during writing or editing of this manuscript.

#### ACKNOWLEDGEMENT

The Authors extend their sincere thanks to the Baba Mastnath University for providing us with an excellent opportunity.

#### COMPETING INTERESTS

Authors have declared that they have no known competing financial interests or non-financial interests or personal relationships that could have appeared to influence the work reported in this paper.

#### REFERENCES

- Abbasi, A., Kurnaz, A., Turhan, Ş., & Mirekhtiary, F. (2020). Radiation hazards and natural radioactivity levels in surface soil samples from dwelling areas of North Cyprus. *Journal of Radioanalytical and Nuclear Chemistry*, 324(1), 203–210. <https://doi.org/10.1007/s10967-020-07027-y>
- Al-Hamarnah, I. F., & Awadallah, M. I. (2009). Soil radioactivity levels and radiation hazard assessment in the highlands of northern Jordan. *Radiation Measurements*, 44(1), 102–110. <https://www.sciencedirect.com/science/article/pii/S135044870800396X>
- Al-Khawlany, A. H., Khan, A., & Pathan, J. (2018). Review on studies in natural background radiation. *Radiation Protection and Environment*, 41(4), 215–222. [https://doi.org/10.4103/rpe.RPE\\_50\\_18](https://doi.org/10.4103/rpe.RPE_50_18)
- Al-Khawlany, A. H., Khan, A., Pathan, J., & Fatema, I. (2020). Assessment of potential radiological risks due to natural gamma radiations in some selected rock samples using  $\gamma$ -ray spectrometry. *Journal of Physics: Conference Series*, 1644(1), 012004. <https://doi.org/10.1088/1742-6596/1644/1/012004>
- Alwaeli, M., & Mannheim, V. (2022). Investigation into the current state of nuclear energy and nuclear waste management—A state-of-the-art review. *Energies*, 15(11), 4275. <https://doi.org/10.3390/en15114275>
- Beretka, J., & Mathew, P. J. (1985). Natural radioactivity of Australian building materials, industrial wastes and by-products. *Health Physics*, 48(1), 87–95. <https://doi.org/10.1097/00004032-198501000-00007>
- Bossey, P., Cinelli, G., Hernández-Ceballos, M., Cernohlawek, N., Gruber, V., Dehandschutter, B., Menneson, F., Bleher, M., Stöhlker, U., Hellmann, I., & et al. (2017). Estimating the terrestrial gamma dose rate by decomposition of the ambient dose equivalent rate. *Journal of Environmental Radioactivity*, 166, 296–308. <https://doi.org/10.1016/j.jenvrad.2016.05.015>
- Darwish, D. A. E., Abul-Nasr, K. T. M., & El-Khayatt, A. M. (2015). Assessment of natural radioactivity and its associated radiological hazards and dose parameters in granite samples from South Sinai, Egypt. *Journal of Radiation Research and Applied Sciences*, 8(1), 17–25. <https://doi.org/10.1016/j.jrras.2014.10.002>
- Del Monte, O., Paola, A., Pérez, B., Sajo-Bohus, L., & Palacios Fernández, D. (2024). Mapping the spatial distribution of natural gamma dose rates as a baseline study in the Province of Asti, Italy. *Pollutants*, 4(2), 174–186.
- Delacroix, D., Guerre, J. P., Leblanc, P., & Hickman, C. (2002). Radionuclide and radiation protection data handbook 2002. *Radiation Protection Dosimetry*, 98(1), 1–168. <https://doi.org/10.1093/oxfordjournals.rpd.a006700>
- Egidi, P. (1997). *Introduction to naturally occurring radioactive material* (Technical Report). Oak Ridge National Laboratory.

- European Commission. (1999). *Radiation protection 112: Radiological protection principles concerning the natural radioactivity of building materials*. Luxembourg: EC.
- ICRP. (1991). *1990 Recommendations of the International Commission on Radiological Protection* (ICRP Publication 60). *Annals of the ICRP*, 21(1–3).
- Johansson, T. B., & Steen, P. (2022). *Radioactive waste from nuclear power plants*. University of California Press.
- Kanse, S. D., Sahoo, B. K., Sapra, B. K., Gaware, J. J., & Mayya, Y. S. (2013). Powder sandwich technique: A novel method for determining the thoron emanation potential of powders bearing high  $^{224}\text{Ra}$  content. *Radiation Measurements*, 48, 82–87. <https://doi.org/10.1016/j.radmeas.2012.11.007>
- Kant, K., Gupta, R., Kumari, R., Gupta, N., & Garg, M. (2015). Natural radioactivity in Indian vegetation samples. *International Journal of Radiation Research*, 13(2), 143–150.
- Khan, H. A. A., & Alshukri, A. S. (2020). Evaluation of environmental and health risks related with the management of medical waste in Al Najaf City. *Journal of Engineering Science and Technology*, 15(5), 4383–4391.
- Kovler, K., Friedmann, H., Michalik, B., Schroeyers, W., Tsapalov, A., Antropov, S., Bituh, T., & Nicolaidis, D. (2017). Basic aspects of natural radioactivity. In W. Schroeyers (Ed.), *Naturally occurring radioactive materials in construction* (pp. 13–36). Elsevier. <https://doi.org/10.1016/B978-0-08-102009-8.00002-6>
- Lolila, F., & Mazunga, M. S. (2023). Measurements of natural radioactivity and evaluation of radiation hazard indices in soils around the Manyoni uranium deposit in Tanzania. *Journal of Radiation Research and Applied Sciences*, 16(1), 100524. <https://doi.org/10.1016/j.jrras.2023.100524>
- Malikova, I., Strakhovenko, V., & Ustinov, M. (2020). Uranium and thorium contents in soils and bottom sediments of Lake Bolshoye Yarovoye, western Siberia. *Journal of Environmental Radioactivity*, 211, 106048. <https://doi.org/10.1016/j.jenvrad.2019.106048>
- Mamont-Ciesla, K., Gwiazdowski, B., Biernacka, M., Zak, A., & Puziewicz, A. (1982). Radioactivity of building materials in Poland. *Journal of Radioanalytical Chemistry*, 70(1–2), 157–166. <https://doi.org/10.1007/BF02516912>
- Martin, J. E. (2006). *Physics for radiation protection: A handbook*. John Wiley & Sons.
- Menon, S., & Kumar, L. S. V. (2019). Weaponizing radioactive medical waste—The looming threat. *International Journal of Nuclear Security*, 5(1), 4. <https://doi.org/10.7290/ijns050104>
- Missimer, T. M., Teaf, C., Maliva, R. G., Danley-Thomson, A., Covert, D., & Hegy, M. (2019). Natural radiation in the rocks, soils, and groundwater of Southern Florida with a discussion on potential health impacts. *International Journal of Environmental Research and Public Health*, 16(11), 1793. <https://doi.org/10.3390/ijerph16111793>
- Musa, I. S. M. (2019). Environmental radiation: Natural radioactivity monitoring. In M. H. Abdel-Dayem (Ed.), *Ionizing and non-ionizing radiation*. IntechOpen. <https://doi.org/10.5772/intechopen.84643>
- Omori, Y., Tokonami, S., Sahoo, S. K., Ishikawa, T., Sorimachi, A., Hosoda, M., Kudo, H., Pornnumpa, C., Nair, R. R. K., Jayalekshmi, P. A., & et al. (2016). Radiation dose due to radon and thoron progeny inhalation in high-level natural radiation areas of Kerala, India. *Journal of Radiological Protection*, 37(1), 111–122. <https://doi.org/10.1088/1361-6498/37/1/111>
- Patel, K. S., Sharma, S., Maity, J. P., Martín-Ramos, P., Fiket, Ž., Bhattacharya, P., & Zhu, Y. (2023). Occurrence of uranium, thorium and rare earth elements in the environment: A review. *Frontiers in Environmental Science*, 10, 1058053. <https://doi.org/10.3389/fenvs.2022.1058053>
- René, M., & Akitsu, T. (2017). Nature, sources, resources, and production of thorium. In *Descriptive inorganic chemistry researches of metal compound* (pp. 201–212).
- Rühm, W., Azizova, T., Bouffler, S., Cullings, H. M., Grosche, B., Little, M. P., Shore, R. S., Walsh, L., & Woloschak, G. E. (2018). Typical doses and dose rates in studies pertinent to radiation risk inference at low doses and low dose rates. *Journal of Radiation Research*, 59(suppl\_2), ii1–ii10. <https://doi.org/10.1093/jrr/rry001>

- Sahoo, B. K., Agarwal, T. K., Gaware, J. J., & Sapra, B. K. (2014). Thoron interference in radon exhalation rate measured by solid state nuclear track detector based can technique. *Journal of Radioanalytical and Nuclear Chemistry*, 302(3), 1417–1420. <https://doi.org/10.1007/s10967-014-3502-6>
- Sahoo, B. K., Nathwani, D., Eappen, K. P., Ramachandran, T. V., Gaware, J. J., & Mayya, Y. S. (2007). Estimation of radon emanation factor in Indian building materials. *Radiation Measurements*, 42(8), 1422–1425. <https://doi.org/10.1016/j.radmeas.2007.05.016>
- Sahoo, P., & Joseph, J. (2021). Radioactive hazards in utilization of industrial by-products: Comprehensive review. *Journal of Hazardous, Toxic, and Radioactive Waste*, 25(4), 03121001. [https://doi.org/10.1061/\(ASCE\)HZ.2153-5515.0000586](https://doi.org/10.1061/(ASCE)HZ.2153-5515.0000586)
- Shankamma, K., Nagaraja, K., Sathish, L. A., & Kumar, K. C. (2022). A review on natural gamma radiation dose levels and its health effects. *International Journal of Health and Allied Sciences*, 11(1), 1.
- Shapiro, J. (2002). *Radiation protection: A guide for scientists, regulators, and physicians*. La Editorial UPR.
- Till, J. E., & Grogan, H. A. (2008). *Radiological risk assessment and environmental analysis*. Oxford University Press.
- Tye, A., Milodowski, A., & Smedley, P. (2017). *Distribution of natural radioactivity in the environment*. British Geological Survey.
- United Nations Scientific Committee on the Effects of Atomic Radiation (UNSCEAR). (2020). *Sources and effects of ionizing radiation: Report to the General Assembly, with scientific annexes (E.00.IX.3)*. United Nations.
- UNSCEAR. (2000). *Sources and effects of ionizing radiation: Report to the General Assembly, with scientific annexes*. United Nations.
- Zanin, Y. N., Zamirailova, A., & Eder, V. (2016). Uranium, thorium, and potassium in black shales of the Bazhenov Formation of the West Siberian marine basin. *Lithology and Mineral Resources*, 51(1), 74–85. <https://doi.org/10.1134/S0024490216010124>

**Disclaimer/Publisher's Note:** The statements, opinions and data contained in all publications are solely those of the individual author(s) and contributor(s) and not of the publisher and/or the editor(s). This publisher and/or the editor(s) disclaim responsibility for any injury to people or property resulting from any ideas, methods, instructions or products referred to in the content.

© Copyright (2025): Author(s). The licensee is the journal publisher. This is an Open Access article distributed under the terms of the Creative Commons Attribution License (<http://creativecommons.org/licenses/by/4.0>), which permits unrestricted use, distribution, and reproduction in any medium, provided the original work is properly cited.

Peer-review history:

The peer review history for this paper can be accessed here:

<https://pr.sdiarticle5.com/review-history/144087>